Quantification of Amine- and Alcohol-Containing Metabolites in Saline Samples Using Pre-extraction Benzoyl Chloride Derivatization and Ultrahigh Performance Liquid Chromatography Tandem Mass Spectrometry (UHPLC MS/MS)

Brittany Widner,* Melissa C. Kido Soule, Frank Xavier Ferrer-González, Mary Ann Moran, and Elizabeth B. Kujawinski

Read Online

ACCESS | Metrics & More | Article Recommendations | SI Supporting Information

ABSTRACT: Dissolved metabolites serve as nutrition, energy, and chemical signals for microbial systems. However, the full scope and magnitude of these processes in marine systems are unknown, largely due to insufficient methods, including poor extraction of small, polar compounds using common solid-phase extraction resins. Here, we utilized pre-extraction derivatization and ultrahigh performance liquid chromatography electrospray ionization tandem mass spectrometry (UHPLC-ESI-MS/MS) to detect and quantify targeted dissolved metabolites in seawater and saline culture media. Metabolites were derivatized with benzoyl chloride by their primary and secondary amine and alcohol functionalities and quantified using stable isotope-labeled internal standards (SIL-ISs) produced from $^{13}C_6$-labeled benzoyl chloride. We optimized derivatization, extraction, and sample preparation for field and culture samples and evaluated matrix-derived biases. We have optimized this quantitative method for 73 common metabolites, of which 50 cannot be quantified without derivatization due to low extraction efficiencies. Of the 73 metabolites, 66 were identified in either culture media or seawater and 45 of those were quantified. This derivatization method is sensitive (detection limits = pM to nM), rapid (∼5 min per sample), and high throughput.
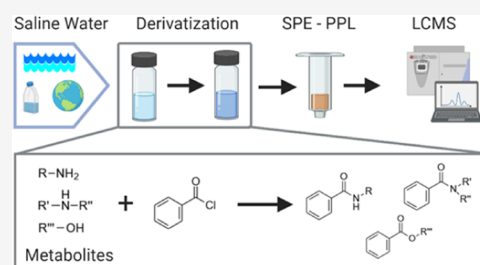
INTRODUCTION

Metabolomics is the study of all molecules produced as a result of cellular metabolism in a biological or environmental system. In aquatic environments, dissolved ("extracellular") metabolites are the chemical currencies that link organisms across trophic levels and spatial and temporal scales.[1] They satisfy nutritional and energetic demands of cells[1−5] and promote interactions within and between taxa.[4,6,7] All marine organisms, from prokaryotes[8] to animals,[9] release metabolites into seawater, and differential metabolite release can reflect the nutritional status as well as cell death via viral lysis, grazing, predation, and apoptosis.[10] Qualitative and quantitative assessments of these processes therefore require the identification and quantification of dissolved metabolites in the seawater matrix.

Dissolved marine metabolites are challenging to quantify due to their high variability in structure and polarity. Metabolites can be bases (e.g., polyamines) or acids (e.g., carboxylic acids), exhibit negative (e.g., phosphates), positive (e.g., amines), or neutral (e.g., carbohydrates) charges, range in size from 50 to >1000 amu, and vary in aromaticity and heteroatom composition. Metabolite analysis in seawater is particularly challenging because of high levels of inorganic salts (mM) relative to analytes (μM to fM). As a result, historical methods targeted groups of related molecules, including amino acids,[11] the B vitamins,[12] and sugars.[13] While effective for the targeted molecules, these piecemeal approaches are time consuming, fall short for molecules that resist strict classification, and do not facilitate the identification of novel compounds.

Current methods in marine dissolved metabolomics seek to identify and quantify tens to hundreds of compounds with varying physicochemical properties in diverse sample types often using mass spectrometry (MS).[14−16] Prior to MS analysis, dissolved metabolites must be extracted from seawater to remove salts. Solid-phase extraction (SPE) using the aromatic PPL resin is a common approach for isolating dissolved organic matter (DOM) from seawater[17] that has been applied to dissolved metabolites.[14,16] PPL cartridges are commercially available and high throughput, but PPL extraction suffers from a significant bias that varies by matrix

and compound type.[18,19] Compound-specific PPL extraction efficiencies in seawater and culture media range from 0 to 100%, with efficiencies <1% for most metabolites tested, particularly small polar biomolecules.[16] Metabolite extraction with PPL also requires relatively large sample volumes (>100 mL for culture media and up to 10 L of seawater from the deep ocean, per replicate). High volume requirements and poor PPL extraction efficiencies have limited studies of dissolved metabolites in marine systems and cultures.

Liquid chromatography (LC) coupled to electrospray ionization (ESI) is commonly used to introduce metabolites into mass spectrometers, where signal intensity depends on analyte concentration and ionization efficiency. However, matrix components can inhibit (or enhance) analyte ionization efficiency, resulting in quantification errors.[20] For example, many small, polar metabolites are poorly retained on widely used reversed-phase (RP) columns leading to coelution between analytes and with salts. Internal standards (ISs) can correct for matrix-related effects. The ideal IS is a stable isotopically labeled (SIL-IS) analyte analogue that experiences the same ionization environment.[21] When isotopologues are not available, matrix effects can be somewhat ameliorated using matrix-matched standard curves, the standard addition method (SAM), or by normalization of samples and standards to similar, but not analyte-paired, SIL-IS.[22] These approaches, however, have limitations. Matrices with sufficiently low background analyte concentrations are challenging to procure, particularly for picomolar metabolites in offshore marine systems. The SAM requires many replicates and produces less precise but sometimes more accurate results than an external or matrix-matched calibration curve.[23] Finally, the use of alternate SIL-ISs may introduce biases if SIL-ISs are not carefully selected.[24]

Functional group derivatization can improve analysis of elusive chemical species. Sogin et al.[15] used derivatization to measure metabolites by gas chromatography (GC)-MS in a culture medium and sediment porewaters. This method uses convenient sample volumes (1 mL), but the detection limits (DLs) (mid to high nM) are likely not sensitive enough for open waters, where metabolites may range from fM to low nM.[2,11] Other studies proposed that ~95% of the human metabolome can be measured by derivatizing four "sub-metabolomes" of amine/phenolic alcohol, carboxylic acids, carbonyl, and alcohol functionalities with dansyl reagents.[25] Derivatization can increase sensitivity by enhancing ionization efficiency and improving chromatographic retention and separation.[26,27] Derivatization can improve absolute and relative quantification by creating analyte-paired SIL-IS.[28] Aqueous derivatization protocols exist for amine groups,[27] but comparable protocols for alcohols are rare, as many alcohol derivatization reagents react explosively with water.[29] Benzoyl chloride (BC) can derivatize (benzoylate) amines (primary and secondary) and alcohol groups into amides and esters, respectively, via a base-catalyzed Schotten–Baumann reaction (Figure S1). BC-based derivatization has been applied widely in biochemical and environmental settings.[30−42] BC reacts quickly in aqueous and organic solution at room temperature and is available in isotopically labeled forms, enabling the use of paired SIL-IS. Benzoyl derivatives are stable in cold storage and in the light[40] and can be detected with ultrahigh performance liquid chromatography (UV−HPLC), LCMS, and GC-MS. For molecules with multiple derivatizable functional groups, BC methods can produce single- or

multilabeled derivatives by modification of derivatization[37] or extraction[34] procedures.

Here, we present a method that pairs BC derivatization with SPE-PPL and UHPLC-ESI-MSMS to quantify small polar metabolites in seawater and saline culture media containing primary and secondary amine and alcohol functionalities (Figure 1). We optimized pH, reagent composition and
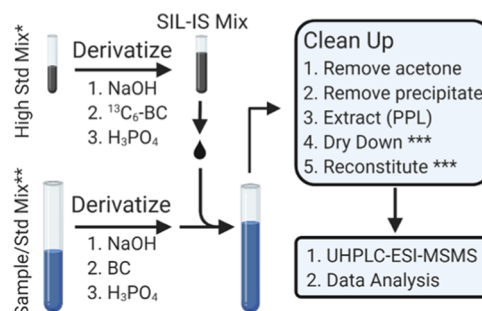
Figure 1. Method overview. *The standard mix for SIL-ISs is prepared in the same matrix as the standard curve. **Standard (Std) mixes for the calibration curve are prepared immediately prior to derivatization. Standards (for SIL-IS and calibration curve) and samples are derivatized simultaneously, and identical aliquots of the SIL-IS mix are added to samples and calibration standards following H_3PO_4 addition. ***Dry down and reconstitution include "washing" to remove precipitate in sample volumes ≥10 mL.

concentration, buffer type, and extraction for saline samples, with analyte-paired SIL-IS produced from $^{13}C_6$-labeled BC. We quantified matrix-derived biases (process effects) for 73 metabolites and established their detection limits, from pM to nM. This method is high throughput because the initial sample processing is fast (5 min per sample when running batches) and requires low sample volumes (1−25 mL, depending on the sample type). BC derivatization improves chromatographic performance, relative to methods without derivatization. Together, these improvements expand the suite of marine dissolved metabolites accessible by LCMS.

■ EXPERIMENTAL SECTION

Chemicals and Standards. Hydrochloric acid (HCl), acetone, methanol, acetonitrile (ACN), and formic acid were purchased from Fisher Scientific (Optima), as were BC (99%, ACROS Organics) and sodium hydroxide (NaOH). Phosphoric acid (85%, ACS reagent grade) was purchased from Sigma-Aldrich. SIL-IS derivatives were prepared with either D_5-BC (99% atom D) or $^{13}C_6$-ring-BC (99% atom ^{13}C) purchased from Cambridge Isotopes and Sigma-Aldrich, respectively. Standards were purchased from Sigma-Aldrich except for 2,3-dihydroxypropane-1-sulfonate (DHPS) obtained by custom synthesis. Deionized (DI) water was obtained from a Milli-Q system (Millipore; resistivity 18.2 MΩ at 24 °C, TOC < 1 μM). Samples and reagents were stored in acid-washed, combusted (at least 4 h at 450 °C), or solvent-rinsed (3× each methanol, acetone, dichloromethane) glassware. BC and all solvents were transferred using solvent-rinsed glass syringes with metal needles (Hamilton). Primary stocks and mixes were stored at −20 °C. The working reagent (5% BC in acetone) was prepared fresh daily.

Sample Collection. Filtered (0.2 μm, poly-(tetrafluoroethylene) (PTFE)) seawater collected from two locations (Vineyard Sound, MA, and the Bermuda Atlantic

Table 1. Method Parameters and Detection Limits for Benzoylated Metabolites

Compound		LCMS Parameters				Detection Limit (nM)		
	Polarity	RT (min)	Precursor (m/z)	Product 1 (m/z)	Product 2 (m/z)	BATS	T. pseudonana	R. pomeroyi
(6R)-5,6,7,8-tetrahydrobiopterin[1]	+	2.7*	346.1510	105.0330	270.0964	NaN	3.6[b]	22[a]
2′deoxycitidine[1]	−	7.7*	330.1095	197.0703	287.1306	0.14[a]	19[a]	NaN
2′deoxyguanosine[1]	−	8.5*	370.1157	121.0281	150.0406	0.052[a]	0.85[a]	0.68[b]
2′deoxyuridine[1]	−	8.5*	331.0935	136.8930	121.0290	NaN	3.9[b]	21[a]
3′AMP[1,*]	+	5	452.0966	105.0330	136.0618	0.0091[b]	0.088[a]	0.45[a]
4-aminobenzoic acid[1]	+	7.8	242.0812	105.0328	NaN	0.14[a]	22[a]	0.91[a]
5′UMP[1,*]	−	6.5	427.0548	78.9586	NaN	0.018[a]	18[α,a]	3.1[α,b]
5′AMP[1,*]	−	6.7	450.0820	134.0456	78.9579	0.034[a]	26[α,a]	18[α,a]
5′deoxyadenosine[1,*]	−	6.1	354.1208	238.0727	NaN	NaN	12[a]	NaN
adenine[1,*]	+	7.4	240.0880	105.0328	137.0449	0.17[α,a]	18[a]	13[b]
adenosine[0]	+	1.7	268.1042	136.0615	NaN	0.16[a]	28[a]	26[a]
alanine[1,*]	−	6.6	192.0666	148.0762	120.0443	0.069[b]	22[α,b]	16[a]
amMP[1,*]	+	3.7	243.1240	122.0714	81.0445	0.030[a]	11[b]	9.3[b]
arginine[1,*]	−	3.3	277.1306	191.1167	120.0443	0.065[a]	8.4[a]	0.95[b]
asparagine[1,*]	−	3.4	235.0724	114.0182	96.0086	0.041[a]	2.1[b]	0.60[b]
aspartate [1,*]	+	4.5	238.0710	105.0328	95.0484	0.24[a]	1.3[b]	1.2[b]
chitobiose[1,*]	+	7.0*	529.2028	126.0543	204.0860	NaN	14[a]	35[a]
chitotriose[1]	+	7.0*	732.2822	126.0543	138.0550	0.016[a]	22[a]	0.44[α,a]
ciliatine[1,*]	+	3	230.0577	105.0328	95.0484	0.016[b]	0.035[b]	0.15[b]
citrulline[1,*]	+	4.6	280.1292	105.0328	113.0702	0.079[a]	1.3[b]	1.2[a]
cysteate[1,*]	−	2.8	272.0234	149.9958	80.9645	0.019[a]	0.42[a]	0.63[b]
cysteine[1,γ]	+	11.2	449.0846	105.0330	224.0368	0.018[b]	0.38[b]	1.1[a]
cytidine[1]	+	7.1*	348.1190	105.0330	216.0765	0.045[a]	26[a]	NaN
cytosine[1,*]	+	7.4	216.0767	105.0328	95.0484	NaN	67[a]	20[b]
desthiobiotin[0]	+	7.3	215.1390	179.1161	197.1281	NaN	0.67[α,b]	0.89[α,a]
DHPS[1,*]	−	5.4	259.0282	121.0285	NaN	0.0056[b]	0.49[a]	0.12[b]
ectoine[1,*,γ]	+	5.4	265.1187	105.0330	98.0596	0.077[a]	8.4[a]	40[a]
Folate[1]	−	7.5	544.1586	325.1192	240.0646	NaN	0.13[α,b]	4.1[α,b]
GABA[1,*]	+	6.8	208.0968	105.0328	95.0484	0.041[a]	0.22[b]	0.15[b]
glucosamine-6-phosphate[1,*]	−	2.4	362.0646	78.9579	96.9681	NaN	1.4[α,a]	5.0[b]
glutamic acid[1,*]	+	5.5	252.0866	105.0328	84.0440	0.095[a]	2.2[b]	4.2[b]
glutamine[1,*]	−	3.8	249.0881	120.0443	187.0880	0.067[a]	1.3[b]	0.48[a]
glycine[1,*]	−	4.3	178.0510	132.0438	134.0607	0.051[a]	87[a]	0.16[b]
glyphosate[1]	−	2.1	272.0329	149.9945	62.9635	NaN	5.3[b]	1.6[b]
guanine[1,*]	+	7.5	256.0829	105.0328	238.0705	NaN	62[a]	73[α,a]
guanosine[1]	+	8.2	388.1251	105.0328	152.0556	0.019[b]	0.56[b]	14[a]
HET[1]	+	12.3	248.0740	188.0352	105.0328	0.30[a]	52[a]	51[a]
histidine[1]	−	2.7	258.0884	120.0443	81.0452	0.14[a]	12[a]	0.94[a]
HMP[1,*]	+	6.3	244.1080	105.0330	123.0456	0.016[b]	0.33[a]	NaN
homoserine[1,*]	−	4.2	222.0772	120.0449	178.0872	0.051[b]	0.12[b]	1.2[a]
homoserine betaine[1,*]	+	5	266.1387	105.0330	207.0643	NaN	0.92[b]	1.9[b]
inosine[1]	−	7.6	371.0997	121.0289	177.0408	0.043[a]	0.42[a]	19[a]
isethionate[1,*]	−	6.4	229.0176	121.0289	NaN	0.040[a]	0.26[a]	0.076[b]
isoleucine[1]	−	11.4	234.1136	190.1247	82.0660	0.050[a]	7.8[a]	0.61[a]
kynurenine[1]	−	11.2	311.1037	128.0492	144.0453	0.015[a]	1.5[b]	5.2[b]
leucine[1]	−	11.2	234.1136	190.1219	82.0652	0.042[a]	1.9[a]	0.28[b]
lysine[2,*]	−	11	353.1507	120.0443	188.1060	0.038[a]	3.4[b]	5.9[a]
malic acid[1,*]	−	7.8	237.0404	121.0290	70.0130	0.044[b]	27[α,a]	1.7[α,a]
methionine[1,*]	+	9.4	254.0845	160.0762	105.0329	NaN	NaN	25[a]
MTA[0,γ]	+	1.6*	314.0918	136.0616	97.0282	NaN	1.2[α,a]	NaN
muramic acid[1,*,γ]	+	6.4*	338.1239	105.0330	200.0704	0.051[b]	0.81[a]	0.15[a]
N-acetyl-D-glucosamine[1,*]	+	7.1*	326.1234	126.0539	105.0330	NaN	0.43[α,a]	9.3[α,a]
N-acetyl-muramic acid[1,γ]	+	8.1*	380.1338	105.0330	126.0543	0.047[a]	0.23[a]	8.0[a]
ornithine[2,*]	+	10.4	341.1496	105.0330	174.0911	0.081[a]	1.5[b]	0.79[a]
pantothenic acid[1]	−	10.8	322.1296	121.0289	128.0711	0.0015[b]	0.086[a]	0.014[b]
phenylalanine[1]	+	11.7	270.1125	105.0328	120.0800	0.069[a]	0.68[b]	0.15[b]
proline[1,*]	−	7.8	218.0823	146.0608	172.0766	0.085[a]	4.2[b]	1.8[a]
putrescine[2,*]	−	11.2	295.1452	120.0442	174.0911	0.0078[b]	0.38[a]	0.096[a]
pyridoxine[1]	+	7.3	274.1074	105.0330	256.0957	NaN	0.33[a]	22[a]

Table 1. continued

	LCMS Parameters					Detection Limit (nM)		
Compound	Polarity	RT (min)	Precursor (m/z)	Product 1 (m/z)	Product 2 (m/z)	BATS	T. pseudonana	R. pomeroyi
S-(1,2-dicarboxyethyl) glutathione[1,*]	+	6.5	528.1282	192.0318	105.0330	0.00095[α,b]	NaN	8.4[α,a]
S-(5′adenosyl)-L-homocysteine [0,γ]	+	3.4	505.1511	136.0611	97.0279	NaN	NaN	18[α,a]
sarcosine[1,*]	−	6.2	192.0666	131.0372	146.0608	0.081[a]	0.43[a]	0.38[a]
serine[1,*]	+	3.7	210.0761	105.0328	95.0485	NaN	12[b]	27[a]
spermidine[3,*]	+	12.7	458.2438	162.0911	336.2064	0.014[b]	0.10[b]	0.14[a]
taurine[1,*]	−	3.3	228.0336	106.9800	79.9564	0.042[a]	0.58[a]	0.38[a]
taurocholic acid[0]	−	12	514.2844	514.2844	NaN	NaN	0.41[α,b]	0.049[α,b]
threonine[1,*]	+	5.5	224.0917	105.0329	56.0491	0.15[a]	0.77[b]	0.99[b]
tryptamine[1]	+	12.7	265.1335	105.0330	144.0798	0.00044[b]	71[α,a]	0.38[a]
tryptophan[1]	−	11.4	307.1088	120.0442	134.0606	0.040[a]	12[a]	0.42[a]
tyrosine[1,*]	−	8.4	284.0928	119.0492	120.0442	0.17[a]	15[α,a]	6.0[b]
uridine[1,*]	−	8.1	347.0885	110.0243	121.0289	0.014[a]	0.77[b]	0.25[b]
valine[1,*]	−	9.4	220.0979	176.1062	68.0495	0.10[a]	6.4[b]	0.71[a]
xanthosine[1]	−	8.5	387.0946	151.0247	193.0350	0.049[a]	9.0[a]	31[α,a]

[a]γ Compounds that were not detected as [M + H]⁺ or [M − H]⁻: S-(5′adenosyl)-L-homocysteine, +OH; cysteine, dimer (+H); ectoine gain H_2O (±H); muramic acid lose H_2O (+H); 5′-deoxy-5′-methylthioadenosine oxidized (+H); n-acetyl-muramic acid lose H_2O (+H). * Compounds that cannot be quantified following PPL extraction without derivatization.[16] [0,1,2,3] The number of benzoyl labels on the compound * on retention time (RT) indicates compounds with multiple distinct peaks. In that case, RT is the maximum of the dominant peak. [a] and [b] indicate DLs calculated for the homoscedastic[50] and heteroscedastic[48] cases, respectively. NaN indicates that the DL could not be calculated due to an inadequate standard curve ($R^2 < 0.9$) [α] indicates DL calculated from the raw peak area. All other DLs were calculated from the SIL-IS normalized peak area. Parameters in this table produced the most sensitive detection for each compound. Parameters for the suboptimal ionization mode and number of benzoyl groups are in Table S5.

Time-series Study site (BATS)) and spent media from *Thalassiosira pseudonana* and *Ruegeria pomeroyi* cultures was used. Details on sample collection, culturing, and experimental design are in the Supporting Text(S-Text).

Derivatization. All filtered samples were basified with a solution of 8 M NaOH and derivatized by the addition of the working BC reagent. Because BC is insoluble in water, insoluble "beads" form when added to aqueous samples, and derivatization occurs at the surface of these beads. Samples were vigorously mixed for 5 min (vortex for spent media and repeated inversions for field samples) or until the BC beads disappeared. The samples were then acidified with concentrated phosphoric acid and stored at −20 °C. For 1 mL of spent medium samples, 30 μL of NaOH, 200 μL of working reagent, and 15 μL of phosphoric acid were added, while for 25 mL of seawater samples, 750 μL of NaOH, 5 mL of working reagent, and 375 μL of phosphoric acid were added.

Postderivatization Sample Prep. We removed acetone prior to extraction on the Bond Elut PPL cartridge (Agilent) to minimize its interference with resin adsorption of the derivatives (culture samples in 4 mL vials with vacufuge; field samples in 40 mL vials with N_2 gas). The change in sample mass was used to confirm acetone removal, and acetone was replaced with the equivalent volume of DI water. Upon acetone removal, a large amount of white precipitate formed, which we separated from the liquid by centrifugation at low speed (1000 rcf for 15 min) to avoid glass breakage. Either 1 mL (cultures) or 25 mL (field) of the resulting liquid was transferred onto a preconditioned (6 mL of methanol followed by 24 mL of 0.01 M HCl) 1 g/6 mL of PPL cartridge and gravity-loaded. Samples were eluted by gravity with 1 cartridge volume of methanol. The eluent was evaporated to near-dryness in a vacufuge, resulting in the formation of a white precipitate. Culture samples were immediately reconstituted in 5% ACN/DI, but, due to the higher BC addition, the precipitate in field samples did not completely dissolve in

5% ACN/DI, and so, these samples received additional washing and centrifugation. Specifically, we added 500 μL of 5% ACN/DI to each field sample, vortexed them to distribute the precipitate, and then centrifuged them (1000 rcf for 15 min). Supernatants were transferred to 2 mL of glass vials for vacufuge evaporation (30 °C for 2 h) and then reconstituted in 5% ACN/DI. All reconstituted samples were stored at 4 °C in 2 mL of LC vials with inserts, after the addition of 5 μL of ACN to prevent precipitation during storage. Derivatization and sample preparation protocols, including pictures and video clips, are available online (dx.doi.org/10.17504/protocols.io.-biukkeuw).

Standard Preparation. Metabolite concentrations were determined using matrix-matched calibration curves normalized with analyte-paired SIL-IS. A metabolite standard mix was spiked at varying levels into axenic L1 medium and 1000 m of BATS water for cultures and seawater samples, respectively, and then derivatized in parallel with the samples. SIL-IS mixes were prepared by adding standards to these matrices and derivatizing with $^{13}C_6$-BC. Standards and samples received the same SIL-IS addition for a given experiment immediately post derivatization. For seawater and DI water, duplicate standard curves were prepared from 5 to 1000 pg/mL, each with a 200 pg/mL SIL-IS addition. Preliminary analysis of culture samples indicated a wide range of metabolite concentrations, so we prepared two standard curves in each culture matrix, from 0 to 1000 and 1000 to 60 000 pg/mL, with SIL-IS additions of 100 and 10 000 pg/mL, respectively. Two sets of samples for each culture were prepared, receiving either the low or high SIL-IS addition. The standard addition method (SAM) was tested at BATS using samples from 1, 95, 160, and 200 m, with standard additions of 0, 5, 10, 20, 50, and 100 pg/mL, each with a 200 pg/mL SIL-IS addition. Standard curves were prepared using the SAM in spent media from *T. pseudonana* and *R. pomeroyi* and in each axenic medium blank. See Table S1 for concentrations in nM.

UHPLC-ESI-MSMS and Peak ID. Samples were analyzed with a Vanquish UHPLC system (Thermo Fisher Scientific) coupled via heated electrospray ionization (H-ESI) to an ultrahigh resolution tribrid mass spectrometer, the Orbitrap Fusion Lumos (Thermo Fisher Scientific). The Lumos was operated in full MS mode with data-dependent tandem MS, guided by a list of user-defined parent ions with a retention time (RT) window (full MS/ddMS$_2$ with inclusion list). All data were collected in the orbitrap analyzer; MS data were used for detection and quantification, and MS/MS data were used for identification and confirmation. Detailed instrument parameters are located in the Supporting Text.

Analyte and SIL-IS peaks were integrated using Skyline,[43,44] and target compounds were identified based on the correspondence of precursor m/z, retention time, and at least one unique MS$_2$ fragment determined from a known derivatized standard (Table 1). Metabolites were quantified from the primary adduct of the precursor, which was typically $[M + H]^+$ or $[M - H]^-$ for positive and negative polarities, respectively (Table 1). All subsequent calculations were performed using MATLAB (R2018b, MathWorks).

Calculations. Calibration curves were inspected manually for nonlinearity and outliers. Higher standard concentrations ($\geq\sim$30 000 pg/mL) sometimes caused ion suppression/ enhancement of or by the SIL-IS (Figure S2) and were excluded from the curve. Only matrix-matched curves with at least five concentrations were retained. Analyte concentrations were calculated from SIL-IS normalized curves using raw peak areas normalized to analyte-matched SIL-IS peak areas. If the normalized area exhibited ion suppression/enhancement or the SIL-IS peak was too small, raw peak areas (and non-normalized standard curves) were used (Table 1). Standard curves were required to have an R^2 greater than 0.9 for quantification and between 0.8 and 0.9 for estimation. For the SAM method, curves with at least three concentrations were retained. Analyte concentrations and standard deviations were determined by extrapolating the x-intercept from the linear curve fit of the standard additions and from the confidence interval of the x-intercept, respectively.[23,45] For matrix-matched standard curves, concentrations were adjusted for nonzero analyte signals in the matrix used to prepare the standard curve.

Detection limits (DLs) were defined as the concentration at which the probability of a false positive was 5%.[46] This probability underlies the common definition of limit of detection (LOD = 3× standard deviation of a standard ≤ 10× of the blank),[47] but that definition assumes that the standard curve residuals are not correlated with the standard concentration (homoscedastic) and requires a matrix-matched blank with negligible analyte concentrations.[23] Our data rarely satisfy the latter requirement and satisfy the former only for some metabolites, thus requiring alternative DL calculations. We measured the standard deviation of normalized and raw peak areas for triplicate standards for four concentrations (Figure S3). If the standard deviation was linearly correlated with concentration (heteroscedastic, $R^2 > 0.70$), we calculated the DL by extrapolating the standard deviation to zero using a linear curve fit.[48,49] If the standard deviation was homoscedastic ($R^2 < 0.7$), we calculated the DL from the variability of the standard curve.[50] In both cases, we assumed triplicate samples ($m = 3$).

We conducted experiments for method optimization and evaluated the effect of different matrices on quantification (process effect, PE). Experimental details are in the Supporting Text. Raw peak areas ranged by orders of magnitude, so we introduced a method performance (MP) parameter to compare treatments within an experiment. MP was calculated for each metabolite as the raw peak area (area$_i$) less the mean raw peak area for all treatments ($\overline{\text{area}}$) normalized to the range of peak areas for all treatments. We multiplied this number by 2 to force the MP to range from -1 to 1 when data are symmetrical around the mean (mean = 0; eq 1). The median of all metabolite MPs was used to compare aggregate differences within experiments

$$\text{MP} = \frac{\text{area}_i - \overline{\text{area}}}{\max(\text{area}) - \min(\text{area})} \times 2 \tag{1}$$

For each metabolite, PE was calculated using a modified matrix effect calculation[51] (eq 2, where X and "Ref" are the sample and reference matrices, respectively). PE was determined for raw peak areas as well as SIL-IS normalized peak areas, where the former reflects matrix-specific biases from the entire process (derivatization efficiency, storage, solubility, extraction efficiencies, and chromatographic and ionization effects) and the latter reflects matrix-specific biases upstream of SIL-IS addition (derivatization efficiency). A PE of zero indicates no effect, while a positive or negative PE indicates enhancement or reduction of the signal relative to a reference matrix. PE was calculated using standard curves from 0 to 100 pg/mL (0, 5, 10, 20, 50, and 100 pg/mL) for BATS seawater and from 3500 to 30 000 pg/mL (3500, 7000, 10 000, and 30 000 pgmL) for culture media. The reference matrices for seawater and cultures were seawater from 1000 m and L1 medium, respectively

$$\text{PE} = \frac{\text{slope}_X - \text{slope}_{\text{Ref}}}{\text{mean}(\text{slope}_X, \ \text{slope}_{\text{Ref}})} \times 100\% \tag{2}$$

■ RESULTS AND DISCUSSION

We optimized derivatization, extraction, and instrument parameters to quantify a large number of compounds with high accuracy and sensitivity. Our method optimization prioritized reduced sample volumes, decreased per-sample costs, and increased sample throughput. We used differences in MP to determine the ideal buffer type, solvent, pH, and BC concentrations. For method validation, we evaluated metabolites in both ionization modes (Figures 2 and S4−S12; Tables S2−S4).

Alcohol and amine functionalities require slightly different reaction conditions for optimal recovery of benzoyl deriva-
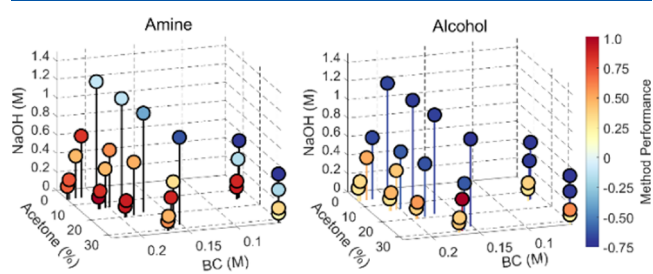
Figure 2. Effect of reagent concentrations on mean method performance (MP) in seawater for compounds with primary or secondary amine (left, $n = 33$) or alcohol (right, $n = 8$) functionalities (Tables S3 and S4). All metabolite concentrations were 100 ng/mL. Derivatives were not observed for BC concentrations <0.05 M.

tives.[37] We generally observed 10−1000× higher raw peak areas for benzoylated amines (amides) than for benzoylated alcohols (esters) at the same metabolite concentration. This may be due to differences in derivatization efficiency, extraction efficiency, derivative solubility, or ionization efficiency. As a result, we prioritized method optimization for alcohols. At high concentrations, we often detected single and multilabeled derivatives for compounds with more than one derivatizable functional group (e.g., double-labeled DHPS; Figure S1), although the method was generally most sensitive for single-labeled compounds (Table 1) regardless of optimization parameters.

Derivatization Optimization. We focused on the following parameters for derivatization optimization: buffer type, reagent (NaOH and BC) concentrations, and organic modifier addition. We compared MPs without a buffer[34] and with tetraborate,[39] phosphate,[37] and carbonate buffers.[40] All metabolites were detected in each treatment, and buffer presence did not drastically alter MP (Figure S4), possibly because seawater and saline culture media are naturally buffered by carbonate. We recommend omitting buffer in saline samples, but a buffer may improve result consistency in fresher water.

We tested the effect of dissolving BC in different organic solvents. Acetonitrile and methanol have been used to derivatize amine and phenolic alcohol metabolites[40] and polyamines,[31] respectively, although other studies added BC directly to aqueous samples without an organic solvent.[34] Acetonitrile is not well miscible with seawater, so we compared methanol and acetone as organic modifiers. Despite large variability in MP for different metabolites, we observed a higher median MP when BC was dissolved in acetone than in methanol (Figure S5).

BC derivatization initiates under high pH. As the reaction proceeds and protons accumulate, the pH decreases and nucleophiles are increasingly protonated, inhibiting further reaction.[30] During benzoylation, BC reacts with water to form benzoic acid, which is insoluble in water when protonated (pK_a = 4.2) and likely forms the observed white precipitate. We observed this precipitate under low pH (<4.2) and in the absence of organic solvents, which dissolve the precipitate. Precipitate formation occurred at an intermediate NaOH concentration and was coincident with efficient alcohol derivatization (Figure S6). Precipitation facilitates pre-extraction removal of excess reagent as benzoic acid, thereby reducing SPE overloading and accumulation on downstream instrumentation.

We determined the optimal MP with respect to all reagent (NaOH, BC, and acetone) concentrations and metabolite functionalities in seawater and spent medium (Figures 2 and S7; Table S2). In both matrices, MP was optimal at ∼0.1 to 0.2 and 0.2 to 0.4 M NaOH for amine and alcohol derivatives, respectively, with a sharp decline in MP at higher NaOH concentrations (>0.6 and >0.4 M for amine and alcohol derivatives, respectively). This trend was particularly pronounced for alcohol derivatives. At optimal NaOH concentrations, MP was stable with respect to BC concentrations between 50 and 250 mM for alcohol- and amine-containing metabolites. MP was stable across acetone concentrations for alcohol functionalities but was slightly higher below ∼20 to 30% acetone for amine derivatives in both matrices. We recommend reagent concentrations of 0.2 M NaOH, 15% acetone, and 70 mM BC for both sample types. These

concentrations maximize MP while minimizing BC concentration and reducing benzoic acid formation.

Postderivatization Sample Prep. We evaluated pre-extraction acetone removal and sample acidification, as both influence derivative and benzoic acid solubilities and could improve PPL extraction efficiency. Upon acetone removal, the quantity of precipitate increased substantially, and we could remove a large fraction before SPE loading. Pre-extraction acetone removal increased the raw peak area of all metabolites up to 60× in seawater and 26× in spent medium (medians = 2.4× and 2.1×, respectively). The median MP did not vary greatly with pH (Figure S8), and derivatives were detected at all pH levels tested (1−5). Acetone removal and acidification likely increased extraction efficiency by reducing benzoic acid overloading on the resin, increasing analyte interactions with the solid phase relative to the liquid phase (acetone), and enhancing protonation of negatively charged groups, such as carboxylic acids.[17]

We recommend extracting 10 and 25 mL for culture and seawater samples, respectively, with a 1 g PPL cartridge (S-Text; Figures S9−S11). These sample volumes are slightly higher than volumes used for GC-MS analysis (1 mL)[15] and 10−100× lower than those required for LCMS metabolite analysis without derivatization (4−10 L).[14] Our method thereby shortens the average field processing times over the PPL method[14] from 60 to 5 min per sample, substantially increasing sample throughput. We determined the optimal reconstitution conditions by varying the ACN concentration added to a 1 mL sample, but we observed chromatographic peak splitting and tailing at CAN >∼15 to 20%. Benzoylated metabolites were observed for all ACN concentrations, with substantial variability in MP across metabolites (Figure S12). In seawater, MP and ACN concentrations were not correlated; in spent medium, the median MP increased slightly with increasing ACN concentration. We recommend reconstituting samples by first washing the precipitate with 5% ACN/water and adding ACN to a final concentration of 10% to prevent precipitation during storage.

UHPLC-ESI-MSMS. Benzoylation improved chromatographic retention of metabolites (Figure 3). Without derivatization, the majority of these metabolites elute early with poor chromatographic resolution, whereas their benzoyl derivatives eluted across the gradient with improved separation (Figure 3). Most derivatives exhibited sharp, well-resolved peaks (Figure S13), although peak tailing was observed for some, particularly early-eluting, phosphate-containing metabolites such as glucosamine-6-phosphate. We recommend monitoring the peak area drift during sample runs using the SIL-IS peak area (Figure S14). A benzoic acid peak was observed at 7.5 min (Figure S15).

Method Accuracy. We improved method accuracy through the use of SIL-ISs and evaluated the effect of matrix-specific biases using process effect (PE). Consistent with previous work, the $^{13}C_6$ SIL-ISs outperformed D_5 SIL-ISs (Table S6), and SIL-IS ion suppression/enhancement of or by the analytes was minimal except at very high concentrations (≥30 000 pg/mL; Figure S2, S-Text). We compared calibration curves prepared with and without normalization to the SIL-IS. For most derivatives, calibration curves were improved (increased R^2) by normalization of the raw peak areas to the SIL-IS peak areas (Figures S16 and S17). For example, of 52 compounds detected with negative polarity, the calibration curves for 33 and 40 compounds were acceptable
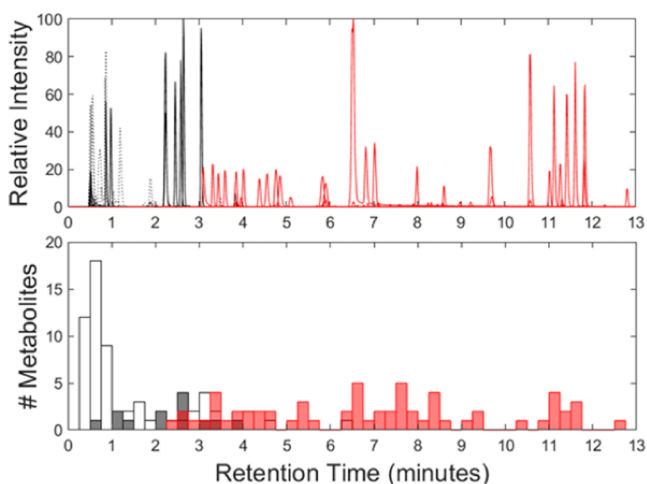
Figure 3. Composite extracted ion chromatograms (EICs; top) and retention times (bottom) of representative metabolites. Red lines and bars represent metabolites that were spiked into seawater, benzoylated, and extracted (*n* = 52). Dotted lines and open bars are the same metabolites in DI that were not derivatized or extracted, while black lines and gray bars represent the subset that can be PPL-extracted from seawater without derivatization (*n* = 13). Concentrations were 100 ng mL^{-1}. No data were recorded during the initial 0.5 min (solvent front) in the top panel. Histogram bins are 0.25 min.

for quantification in seawater and spent medium, respectively, as compared to only 13 and 26 compounds prepared from raw peak areas.

PEs were determined in the two matrix types, where PE indicates enhancement (+PE) or reduction (−PE) of the signal relative to a reference matrix, and a PE of zero indicates no matrix-specific bias. PEs calculated from raw peak areas reflect biases of the entire process, while PEs calculated from SIL-IS normalized peak areas reflect biases in only the derivatization step. For oligotrophic seawater, we calculated PE for samples from four BATS depths (0, 95, 160, 200 m; *n* = 6 per curve) and DI water (*n* = 12) as compared to BATS deep water (1000 m; *n* = 12; Table S3). For cultures, we calculated PE for spent media from *T. pseudonana* and *R. pomeroyi* cultures relative to the axenic medium blanks (L1 and *f*/2 + propionate; Table S4). Fewer compounds could be quantified in DI water than in seawater because these compounds were either not derivatized in DI water or the DI standard curve was inferior (Figure S16 and Table S3). This resulted in only 54 quantifiable compound/polarity pairs (both polarities) for SIL-IS normalized peak areas in DI water compared to 66 in seawater.

In both seawater and culture media, the median PE for all treatments deviated farther from 0 when calculated from raw peak areas (−28 and 17%, respectively) than from SIL-IS normalized peak areas (4.1 and 0.3%; Figures S16 and S17; Tables S3 and S4), indicating that the majority of matrix-specific biases occur downstream of derivatization. In seawater, the PEs for raw peak areas were more negative at shallower depths than at deeper depths and in DI water (Figure S16), indicating relative signal depression in shallow water. This trend may be driven by labile organic matter content, which is higher in shallower, more biologically productive, water than in deep and DI water (Table S7). Organic matter may interfere with extraction or derivative solubility. In both matrix types, the PE of some compounds fell outside the acceptable range (± 20%). Because PE represents a systematic bias, rather than a random error, the concentrations of these metabolites should

be interpreted cautiously. Overall, normalization to the analyte-specific SIL-IS increases the number of quantifiable compounds and reduces the likelihood of systemic biases due to matrix effects.

Method Validation. We compared quantification in five samples using either a matrix-matched calibration curve prepared in freshly collected deep seawater (1000 m at BATS) or the standard addition method (SAM) with both raw and SIL-IS normalized peak areas. We chose deep ocean water because it should have the lowest background of dissolved metabolites and organic carbon (Table S7) with similar pH and ionic strength as shallower water. Indeed, many metabolite concentrations in deep water were lower than those in the shallower depths, although some were still abundant (Table S8). At the shallow depths, calculated metabolite concentrations were similar using the two methods, but the relative standard deviation (RSD) was much higher for concentrations calculated using the SAM, reflecting the higher inherent error of the *x*-intercept relative to a point within the bounds of the calibration curve.[45]

For example, DHPS concentrations calculated from the SIL-IS normalized matrix-matched curve were 0.10 ± 0.01 and 0.35 ± 0.02 nM at 1 and 95 m (RSD = 13 and 4.4%, respectively). Using the SAM, DHPS concentrations were 0.12 ± 0.07 and 0.21 ± 0.11 nM at 1 and 95 m, respectively (RSD = 62 and 51%).

Each method contains a source of inaccuracy: PE in the matrix-matched curve and extrapolation of the *x*-intercept below the known linear range of the calibration curve in the SAM.[23] The SAM also suffers from low precision (RSD)[23] and practical limitations. We used a 6-point curve for the SAM, but in practice, analysts generally use three or four standard additions, optimally with concentrations equal to 1×, 2×, 3×, and 4× the analyte.[45]

Method Sensitivity. Most of our data fell into the case of homoscedastic standard deviation, enabling DL calculations with the method of Vogelgesang and Hädrich.[50] The calculation for the heteroscedastic case[48] generally resulted in a lower DL because it extrapolates below the range of standard deviations observed, rather than using the aggregate standard deviation. Although both calculations minimize biases associated with a nonzero background analyte concentration, as compared to the EPA calculation (LOD),[47] they do not entirely eliminate this bias, particularly if the background concentration is high. This is especially true for the homoscedastic case, where the DL is derived from the aggregate standard deviation for all standard concentrations. Some analyte background concentrations were elevated in the calibration matrices, particularly in culture media, which likely resulted in an overestimation of the DLs. However, because of the poor derivative recovery in DI water (Figure S16 and Table S3), the "zero" background signal cannot be determined.

Our method is more sensitive in oligotrophic seawater than in cultures. DLs ranged from 0.010 to 2 nM for oligotrophic seawater (median 0.079 nM) and 0.081 to 150 nM for culture media (median 2.3 nM; Table 1). This disparity may result from differences in sample volume or type and the more conservative calculation for cultures. While culture media and seawater have similar salinity and pH, DOC concentrations are substantially higher in culture media than in oligotrophic seawater (Table S8), and the DOC character also differs. DOC concentration and character may impact derivatization and extraction[16] efficiencies. For example, phytoplankton release

alcohol-containing polysaccharides,[13] which may compete with metabolites for BC or adhere to the PPL, thereby lowering analyte retention.

Some compounds quantified by our method are also targeted by the PPL method,[16] the GC-MS method,[15] and the *o*-phthalaldehyde (OPA) amino acid method.[11] Our seawater DLs are similar in magnitude to those obtained with underivatized PPL extraction (0.007−2.4 nM)[16] and lower than those reported using a GC-MS derivatization method (60−1000 nM).[15] The DLs we report for culture media are of similar magnitude to those from Sogin et al.[15] The seawater DLs for the 22 amino acids reported here (0.020−0.24 nM) are lower than those of the OPA method (∼0.5 to 1 nM),[11] while the amino acid DLs for cultures are higher (0.12−87 nM), likely due to the conservative nature of that calculation.

The DLs reported here were sufficiently sensitive to quantify numerous metabolites in culture media and at BATS (Table S8). Additional benzoylated metabolites were identified but did not meet the quality threshold for quantification (Table S8), particularly in culture media. These will likely be quantifiable after future method refinements.

CONCLUSIONS

Our pre-extraction benzoylation method is sensitive and robust for the detection and quantification of a broad suite of amine- and alcohol-containing dissolved metabolites in seawater and saline culture media. DLs are nano- to picomolar, and matrix biases are minimal due to the use of matrix-matched calibration curves and analyte-matched SIL-ISs. This method quantifies numerous compounds that have not been previously measured in seawater, limiting the understanding of their role in aquatic systems. For example, sulfonates such as DHPS and isethionate have emerged as key players in marine ecosystems and the sulfur cycle,[4] but, using the existing methodology, these compounds cannot be extracted from saline solution[16] without derivatization. Our method, which is sensitive and precise for both compounds, will facilitate an improved understanding of these processes and others in laboratory studies and in the field.

ASSOCIATED CONTENT

Supporting Information

The Supporting Information is available free of charge at https://pubs.acs.org/doi/10.1021/acs.analchem.0c03769.

Supporting Text and Figures S1−S17 (PDF)

Tables S1−S9 (XLSX)

AUTHOR INFORMATION

Corresponding Author

Brittany Widner − *Department of Marine Chemistry and Geochemistry, Woods Hole Oceanographic Institution, Woods Hole, Massachusetts 02543, United States;* orcid.org/0000-0002-1527-2717; Email: brittany.widner@gmail.com

Authors

Melissa C. Kido Soule − *Department of Marine Chemistry and Geochemistry, Woods Hole Oceanographic Institution, Woods Hole, Massachusetts 02543, United States*

Frank Xavier Ferrer-González − *Department of Marine Sciences, University of Georgia, Athens, Georgia 30602, United States*

Mary Ann Moran − *Department of Marine Sciences, University of Georgia, Athens, Georgia 30602, United States;* orcid.org/0000-0002-0702-8167

Elizabeth B. Kujawinski − *Department of Marine Chemistry and Geochemistry, Woods Hole Oceanographic Institution, Woods Hole, Massachusetts 02543, United States;* orcid.org/0000-0001-8261-971X

Complete contact information is available at:
https://pubs.acs.org/10.1021/acs.analchem.0c03769

Notes

The authors declare no competing financial interest.

REFERENCES

(1) Moran, M. A.; Kujawinski, E. B.; Stubbins, A.; Fatland, R.; Aluwihare, L. I.; Buchan, A.; Crump, B. C.; Dorrestein, P. C.; Dyhrman, S. T.; Hess, N. J.; et al. *Proc. Natl. Acad. Sci. U.S.A.* **2016**, *113*, 3143−3151.

(2) Heal, K. R.; Carlson, L. T.; Devol, A. H.; Armbrust, E. V.; Moffet, J. W.; Stahl, D. A.; Ingalls, A. E. *Rapid Commun. Mass Spectrom.* **2014**, *28*, 2398−2404.

(3) Sañudo-Wilhelmy, S. A.; Gómez-Consarnau, L.; Suffridge, C.; Webb, E. A. *Annu. Rev. Mar. Sci.* **2014**, *6*, 339−367.

(4) Moran, M. A.; Durham, B. P. *Nat. Rev. Microbiol.* **2019**, *17*, 665−678.

(5) Sipler, R. E.; Bronk, D. A. *Biogeochemistry of Marine Dissolved Organic Matter*; Hansell, D. A.; Carlson, C. A., Eds.; Academic Press, 2015; pp 127−232.

(6) van Tol, H. M.; Amin, S. A.; Armbrust, E. V. *ISME J.* **2017**, *11*, 31−42.

(7) Gram, L.; Grossart, H.-P.; Schlingloff, A.; Kiørboe, T. *Appl. Environ. Microbiol.* **2002**, *68*, 4111−4116.

(8) Fiore, C. L.; Longnecker, K.; Kido Soule, M. C.; Kujawinski, E. B. *Environ. Microbiol.* **2015**, *17*, 3949−3963.

(9) Azam, F.; Fenchel, T.; Field, J. G.; Gray, J. S.; Meyer-Reil, L. A.; Thingstad, F. *Mar. Ecol.: Prog. Ser.* **1983**, *10*, 257−263.

(10) Nagata, T. *Microbial Ecology of the Oceans*; Kirchman, D. L., Ed.; Wiley-Liss: New York, 2000; pp 121−152.

(11) Mopper, K.; Lindroth, P. *Limnol. Oceanogr.* **1982**, *27*, 336−347.

(12) Suárez-Suárez, A.; Tovar-Sánchez, A.; Rosselló-Mora, R. *Anal. Chim. Acta* **2011**, *701*, 81−85.

(13) Panagiotopoulos, C.; Sempéré, R. *Limnol. Oceanogr.: Methods* **2005**, *3*, 419−454.

(14) Kido Soule, M. C.; K, L.; W M, J.; Kujawinski, E. B. *Mar. Chem.* **2015**, *177*, 374−387.

(15) Sogin, E. M.; Puskas, E.; Dubilier, N.; Liebeke, M. *mSystems* **2019**, *4*, 1−14.

(16) Johnson, W. M.; Kido Soule, M. C.; Kujawinski, E. B. *Limnol. Oceanogr.: Methods* **2017**, *15*, 417−428.

(17) Dittmar, T.; Koch, B.; Hertkorn, N.; Kattner, G. *Limnol. Oceanogr.: Methods* **2008**, *6*, 230−235.

(18) Longnecker, K.; Soule, M. C. K.; Kujawinski, E. B. *Mar. Chem.* **2015**, *168*, 114−123.

(19) Becker, J. W.; Berube, P. M.; Follett, C. L.; Waterbury, J. B.; Chisholm, S. W.; DeLong, E. F.; Repeta, D. J. *Front. Microbiol* **2014**, *5*, 1−14.

(20) Annesley, T. M. *Clin. Chem.* **2003**, *49*, 1041−1044.

(21) Hewavitharana, A. *Crit. Rev. Anal. Chem.* **2009**, *39*, 272−275.

(22) Boysen, A. K.; Heal, K. R.; Carlson, L. T.; Ingalls, A. E. *Anal. Chem.* **2018**, *90*, 1363−1369.

(23) Andersen, J. E. *TrAC, Trends Anal. Chem.* **2017**, *89*, 21−33.

(24) Tan, A.; Boudreau, N.; Lévesque, A. *LC-MS in Drug Bioanalysis*; Springer, 2012; pp 1−32.

(25) Han, W.; Li, L. *Clinical Metabolomics*; Springer, 2018; pp 213−225.

(26) Barnaby, O. S.; Benitex, Y.; Cantone, J. L.; McNaney, C. A.; Olah, T. V.; Drexler, D. M. *Bioanalysis* **2015**, *7*, 2501−2513.

(27) Qi, B.-L.; Liu, P.; Wang, Q.-Y.; Cai, W.-J.; Yuan, B.-F.; Feng, Y.-Q. *TrAC, Trends Anal. Chem.* **2014**, *59*, 121−132.

(28) Guo, K.; Li, L. *Anal. Chem.* **2009**, *81*, 3919−3932.

(29) Escrig-Doménech, A.; Simó-Alfonso, E.; Herrero-Martínez, J.; Ramis-Ramos, G. *J. Chromatogr. A* **2013**, *1296*, 140−156.

(30) Redmond, J. W.; Tseng, A. *J. Chromatogr. A* **1979**, *170*, 479−481.

(31) Asotra, S.; Mladenov, P. V.; Burke, R. D. *J. Chromatogr. A* **1987**, *408*, 227−233.

(32) Liu, R.; Jia, Y.; Cheng, W.; Ling, J.; Liu, L.; Bi, K.; Li, Q. *Talanta* **2011**, *83*, 751−756.

(33) Gupta, R. N.; Eng, F.; Gupta, M. L. *Clin. Chem.* **1982**, *28*, 32−33.

(34) Holčapek, M.; Virelizier, H.; Chamot-Rooke, J.; Jandera, P.; Moulin, C. *Anal. Chem.* **1999**, *71*, 2288−2293.

(35) Kuribayashi, M.; Tsuzuki, M.; Sato, K.; Abo, M.; Yoshimura, E. *Chromatographia* **2008**, *67*, 339−341.

(36) Nordström, A.; Tarkowski, P.; Tarkowska, D.; Dolezal, K.; Åstot, C.; Sandberg, G.; Moritz, T. *Anal. Chem.* **2004**, *76*, 2869−2877.

(37) Oehlke, J.; Brudel, M.; Blasig, I. E. *J. Chromatogr. B: Biomed. Sci. Appl.* **1994**, *655*, 105−111.

(38) Miyagi, M.; Yokoyama, H.; Hibi, T. *J. Chromatogr. B* **2007**, *854*, 286−290.

(39) Song, P.; Mabrouk, O. S.; Hershey, N. D.; Kennedy, R. T. *Anal. Chem.* **2012**, *84*, 412−419.

(40) Wong, J.-M. T.; Malec, P. A.; Mabrouk, O. S.; Ro, J.; Dus, M.; Kennedy, R. T. *J. Chromatogr. A* **2016**, *1446*, 78−90.

(41) Mishra, S.; Singh, V.; Jain, A.; Verma, K. K. *Analyst* **2001**, *126*, 1663−1668.

(42) Tran, B. N.; Okoniewski, R.; Bucciferro, A.; Jansing, R.; Aldous, K. M. *J. AOAC Int.* **2014**, *97*, 232−237.

(43) Henderson, C. M.; Shulman, N. J.; MacLean, B.; MacCoss, M. J.; Hoofnagle, A. N. *Clin. Chem.* **2018**, *64*, 408−410.

(44) Pino, L. K.; Searle, B. C.; Bollinger, J. G.; Nunn, B.; MacLean, B.; MacCoss, M. J. *Mass Spectrom. Rev.* **2020**, *39*, 229−244.

(45) Danzer, K.; Currie, L. A. *Pure Appl. Chem.* **1998**, *70*, 993−1014.

(46) Currie, L. A. *Anal. Chem.* **1968**, *40*, 586−593.

(47) Boyd, R. K.; Basic, C.; Bethem, R. A. *Trace Quantitative Analysis by Mass Spectrometry*; John Wiley & Sons, 2011.

(48) Zorn, M. E.; Gibbons, R. D.; Sonzogni, W. C. *Environ. Sci. Technol.* **1999**, *33*, 2291−2295.

(49) Griffith, D. R.; Kido Soule, M. C.; Matsufuji, H.; Eglinton, T. I.; Kujawinski, E. B.; Gschwend, P. M. *Environ. Sci. Technol.* **2014**, *48*, 2569−2578.

(50) Vogelgesang, J.; Hädrich, J. *Accredit. Qual. Assur.* **1998**, *3*, 242−255.

(51) Chawla, S.; Patel, H. K.; Gor, H. N.; Vaghela, K. M.; Solanki, P. P.; Shah, P. G. *J. AOAC Int.* **2017**, *100*, 616−623.